Available online at www.sciencedirect.com
SCIENCE DIRECT
Catalysis Today 104 (2005) 267–273
CATALYSIS TODAY
www.elsevier.com/locate/cattod

Compatibility of hydrogen transfer via Pd-membranes with the rates of heterogeneously catalysed steam reforming

Alexandra Kleinert [a,*], Gerd Grubert [a], Xiulian Pan [b], Christof Hamel [c], Andreas Seidel-Morgenstern [c], Jürgen Caro [a]

[a] *Institute of Physical Chemistry and Electrochemistry, University of Hannover, Callinstr. 3–3a, D-30167 Hannover, Germany*
[b] *Fraunhofer Institute for Interfacial Engineering and Biotechnology, Nobelstr. 9, D-70569 Stuttgart, Germany*
[c] *Max Planck Institute for Dynamics of Complex Technical Systems, Sandtorstr. 1, D-39106 Magdeburg, Germany*

Available online 10 May 2005

Abstract

For an effective operation of a membrane reactor in comparison with a conventional fixed-bed reactor, the kinetic compatibility of hydrogen production and its removal is essential. The aim of this work is to provide an estimation of the membrane area needed for the extraction of the hydrogen which is produced at a defined gas hourly space velocity (GHSV) in steam reforming of methane (SR). The SR was studied in a fixed-bed reactor using a conventional Ni-catalyst for evaluating the kinetic parameters. The conversion of methane was simulated by a one-dimensional, non-isothermal reactor model and compared with the experimental results. Hydrogen conducting Pd-membranes were prepared by electroless plating, and the hydrogen permeation through these membranes was determined. The analysis performed can provide an estimation for the design of a catalytic membrane reactor.

Keywords: Pd-membranes; Steam reforming; Gas hourly space velocity

1. Introduction

Catalytic SR is the conversion of hydrocarbons with steam. It is the main technology for the production of syngas ($CO + H_2$) from methane. A conventional SR-catalyst contains nickel supported on modified and promoted Al_2O_3. In this work, a grinded commercial SR-catalyst with a particle size of 0.16–0.40 mm was studied. Industrially, the shapes of the SR-catalyst are Raschig rings or seven-spoked wheels to achieve an acceptable pressure drop and heat transfer [1].

The following reversible reactions are possible in the SR-process, namely the reforming (eqs. (1) and (3)), the water–gas shift (eq. (2)), the Boudouard reaction (eq. (4)), the decomposition of methane (eq. (5)) and the dry-reforming (eq. (6)):

$$CH_4 + H_2O \rightleftharpoons CO + 3H_2, \quad \Delta H^\circ_{298} = 206\,\text{kJ/mol} \tag{1}$$

$$CO + H_2O \rightleftharpoons CO_2 + H_2, \quad \Delta H^\circ_{298} = -41\,\text{kJ/mol} \tag{2}$$

$$CH_4 + 2H_2O \rightleftharpoons CO_2 + 4H_2, \quad \Delta H^\circ_{298} = 165\,\text{kJ/mol} \tag{3}$$

$$2CO \rightleftharpoons C + CO_2, \quad \Delta H^\circ_{298} = -172\,\text{kJ/mol} \tag{4}$$

$$CH_4 \rightleftharpoons C + 2H_2, \quad \Delta H^\circ_{298} = 75\,\text{kJ/mol} \tag{5}$$

$$CH_4 + CO_2 \rightleftharpoons 2CO + 2H_2, \quad \Delta H^\circ_{298} = 247\,\text{kJ/mol} \tag{6}$$

The slightly exothermal water–gas shift reaction (eq. (2)) dominates only at low temperatures ($T < 400\,^\circ\text{C}$). Under industrial conditions, at $T = 900$–$1100\,^\circ\text{C}$ and a pressure of $p = 30$ bar, the water–gas shift reaction becomes less dominant, so that the overall reaction enthalpy is still positive and the reforming process is close to the thermodynamic limitations [1]. Therefore, SR requires a high reaction temperature and, thus, SR is cost-intensive. One possibility to decrease the operational costs is the reduction of the reaction temperature. To overcome the thermodynamic limitations of the SR-process at a lower temperature, one of the products has

* Corresponding author. Tel.: +49 511 762 2942; fax: +49 511 762 19121.
E-mail address: alexandra.kleinert@pci.uni-hannover.de (A. Kleinert).

0920-5861/$ – see front matter © 2005 Elsevier B.V. All rights reserved.
doi:10.1016/j.cattod.2005.03.068

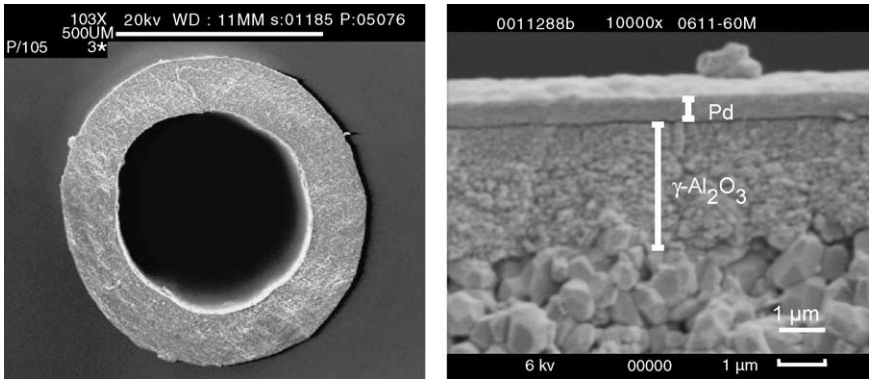

Fig. 1. SEM images of the cross sections of an α-Al_2O_3 capillary at different magnifications. In the right SEM, the 3 μm thick γ-Al_2O_3 intermediate layer and the 0.6 μm thin Pd top-layer can be seen.

to be removed via a membrane [2]. This led to the idea to combine SR with Pd-membranes [3,4] which are widely known as a highly hydrogen selective permeation material [5,6]. The potential benefits of a membrane supported SR are a lower reaction temperature and a higher methane conversion while high purity hydrogen, e.g. for fuel cells, can be delivered. A possible disadvantage of this combination could be a higher coke formation. Jørgensen et al. [7] reported that no coke is formed if the H_2O/CH_4 ratio is at least 2.5 even if hydrogen is removed. For the application of innovative membrane reactors, the compatibility of the amounts of hydrogen produced and removed is essential. Therefore, on the one hand it is necessary to quantify the rates of the SR-reaction for different reaction conditions and thus the amount of hydrogen produced. On the other hand, it is necessary to specify the permeability of the Pd-membrane and the required membrane area.

From the literature, it is known that the presence of carbon monoxide decreases the hydrogen permeation through a palladium membrane because of a blockage of the surface [8]. The lower the temperature the stronger is the influence of this effect. Amandusson et al. [8] found a complete blockage of the palladium at $T = 100$ °C, and therefore, no permeation of hydrogen through the membrane at this temperature. At $T = 250$ °C, they noted a decrease of the flux of only 10% and at temperatures above 350 °C, they found no evidence for any influence of CO at all. In this study, the influence of carbon monoxide at temperatures around 500 °C on the flux of hydrogen has not been investigated.

The hydrogen permeation is a complex process which consists of the adsorption of hydrogen, the dissociation, the diffusion of hydrogen atoms through the metal lattice, the recombination of hydrogen atoms on the low pressure side and the desorption of molecular hydrogen. Generally, the permeation can be described by the following expression [9,10]:

$$J_{H_2} = \frac{Q_{H_2}}{L} \cdot (p^n_{H_2,\mathrm{ret}} - p^n_{H_2,\mathrm{perm}}) \quad (6)$$

with J_{H_2} being the hydrogen flux through the membrane, Q_{H_2} the permeability, L the membrane thickness and p being the hydrogen partial pressure either on the permeate or on the retentate side. In Pd-membranes thicker than 20 μm [11] and 50 μm [12], respectively, the permeation rate is usually controlled by the hydrogen diffusion through the metal lattice, which can be described by Sievert's law [9]:

$$J_{H_2} = \frac{D_{H_2} \cdot K_S}{L} \cdot (p^{0.5}_{H_2,\ \mathrm{ret}} - p^{0.5}_{H_2,\mathrm{perm}}) \quad (7)$$

with K_S being the Sievert's constant [10]. The product of the diffusion coefficient and the Sievert's constant is the permeability coefficient $Q_{H_2,\mathrm{Sievert}}$ [13]. Eqs. (6) and (7) describe the fact that under diffusion controlled conditions the hydrogen flux increases with $1/L$.

In contrast, for thinner membranes, the surface reaction processes gain importance and can become the rate limiting steps, and the flux of hydrogen is proportional to the difference of the partial pressures [3,14]:

$$J_{H_2} = \frac{Q_{H_2,\mathrm{linear}}}{\mathrm{L}} \cdot (p_{H_2,\mathrm{ret}} - p_{H_2,\mathrm{perm}}) \quad (8)$$

with $Q_{H_2,\mathrm{linear}}$ being the permeability coefficient [13].

However, in practice there is an interplay of diffusion and surface control. Obviously, higher hydrogen fluxes can be achieved with thinner membranes. Therefore, Pd-membranes with a thickness of 2–3 μm supported on porous alumina fibres are used in this work. To obtain a high membrane area per module volume, hollow fibre geometry is chosen (Fig. 1).

2. Experimental

2.1. Preparation of Pd-membranes and the permeation study

All chemicals used were purchased from FLUKA (Germany). The α-Al_2O_3 capillary supports, which have been produced by established procedures [15], were homemade. The inner diameter lies in the range of 500–700 μm and the outer diameter in the range of 800–900 μm. The average pore size in the walls was 0.2 μm and the

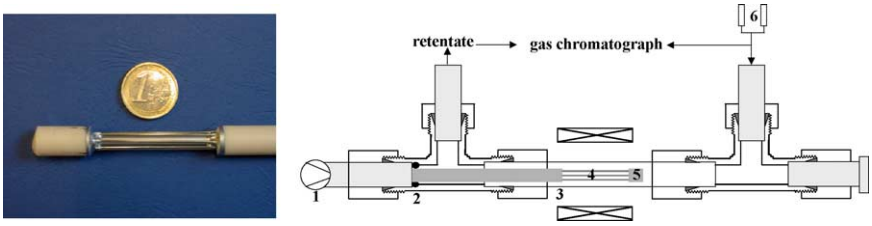

Fig. 2. Hollow fibre module with six capillaries incorporated (left), apparatus for permeation (right): (1) pump for extraction of the permeate; (2) O-ring sealing; (3) quartz reactor; (4) hollow fibres; (5) dead-end of the module; (6) mass flow controller for hydrogen and nitrogen.

porosity 20%. Several capillaries were assembled into modules of different separation area. In the permeation studies shown in this paper, the module comprises six fibres giving a total area of 6.8 cm^2. As shown in Fig. 2, a long dense ceramic tube was used to collect permeating gases at one end of the fibres. At the other end, the fibers were sealed by glaze to assure the connection between ceramic tube and capillaries. The effective length of the fibres was 4.5 cm. Then, an intermediate γ-Al_2O_3 layer and finally the dense Pd layer were deposited directly on the modules. By applying a vacuum-assisted dip-coating technique, a 2–3 μm thick γ-Al_2O_3 layer was deposited onto the outer surface of the capillaries, thus the surface roughness of the substrate was reduced resulting in a pore size of 4–6 nm [16].

A standard autocatalytic electroless plating process [17,18] was applied to the modules after the activation of palladium seeds in the γ-Al_2O_3 layer in an H_2 atmosphere at 200–500 °C to obtain metallic nuclei. The plating bath contained 25 mmol/L $PdCl_2$, 100 mmol/L Na_2[EDTA], 117 g/L $NH_3{\cdot}H_2O$, and 16 g/L $N_2H_4{\cdot}2H_2O$. The pH value of the bath was adjusted to 11 and the temperature was held at 45 °C. Fig. 1 shows SEM images of an α-Al_2O_3 capillary with a 3 μm thick γ-Al_2O_3 intermediate layer and a 0.6 μm thick Pd-membrane layer on top. Surface SEM images (Fig. 1) indicate a continuous and very smooth Pd layer with no noticeable defects and pinholes in the scanned area.

The permeation measurements were carried out in a tubular quartz reactor. The dead end module was sealed by a silicon O-ring (Fig. 2). The module was heated up in nitrogen atmosphere. When the permeation temperature was reached a mixture of hydrogen (purity 99.999%) and nitrogen (purity 99.999%) was fed into the reactor. The permeate was extracted by a pump, the retentate and the feed were analysed with a gas chromatograph (HP 6890N) equipped with a Carboxen-1000 column and a thermal conductivity detector. The fluxes of the feed and the retentate were measured by a flowmeter. The pressure of the retentate and of the permeate was measured with pressure gauges. The temperature (412–528 °C) and the hydrogen partial pressure (0.310–0.810 bar) were varied.

2.2. Kinetic studies on the SR-catalyst

For the SR-catalyst under study, a fixed-bed reactor in co-feed mode was used. The tubular stainless steel reactor had an inner diameter of 7 mm and a total length of 1200 mm. The catalyst packed bed had a length of 130 mm. The catalyst was diluted with SiO_2 in order to avoid hot spots. For temperature measurements, a thermocouple was placed in a quartz tube inside the catalyst bed. The gas flows were controlled by mass flow controllers (Mättig GmbH). Steam was generated from double distilled water in a controlled evaporator unit (CEM, Mättig GmbH) and mixed with helium in a defined ratio.

The kinetic parameters were determined for reaction temperatures, T, of 800, 850 and 900 °C. The catalyst was heated up to the respective temperature in helium/nitrogen atmosphere. When the temperature was achieved, the following reaction gas mixtures containing 3 vol.% methane (purity 99.5%), 10–19 vol.% steam (steam/methane ratios 2.0, 3.3 and 5.0) and 78–87 vol.% of a helium/nitrogen mixture (helium:nitrogen = 9.5:0.5, purity 99.996 and 99.999%) were fed into the reactor. Nitrogen was used as an inert internal standard to consider dilution effects in the reaction gas mixture. In order to get different gas hourly space velocities (GHSV) from 1.0×10^6 to 5.8×10^6 h^{-1}, the mass of the pure catalyst was varied from 6.5 to 404.0 mg and the total gas flows from 450 to 630 mL/min. The GHSV was calculated as:

$$\mathrm{GHSV} = \frac{\dot{V}_{\mathrm{total}}}{V_{\mathrm{catalyst}}} \tag{9}$$

with $\dot{V}_{\mathrm{total}}$ being the total gas flow and V_{catalyst} being the volume of the catalyst.

For each reaction condition, the educts and products were analysed by gas chromatography. The pressures up and down stream of the reactor were controlled by a pressure gauge. The pressure of the feed was around 1.5 bar and the pressure drop over the reactor was approximately 0.07 bar.

The conversion with respect to the methane was calculated as:

$$X_{\mathrm{CH_4}} = \frac{[\mathrm{CO}] + [\mathrm{CO_2}]}{[\mathrm{CO}] + [\mathrm{CO_2}] + [\mathrm{CH_4}]_{\mathrm{out}}} \tag{10}$$

with $[i]$ being the concentration of component i.

The yield of carbon monoxide was calculated as:

$$Y_{\mathrm{CO}} = \frac{[\mathrm{CO}]}{[\mathrm{CH_4}]_{\mathrm{in}}} \cdot 100 \tag{11}$$

The selectivity of carbon monoxide formation was calculated as:

$$S_{CO} = \frac{[CO]}{[CO] + [CO_2]} \quad (12)$$

The selectivity of carbon dioxide formation was determined $S_{CO_2} = 1 - S_{CO}$. The carbon balance in the experiments performed was $(100 \pm 4)\%$.

3. Results and discussions

3.1. Permeation

Fig. 3 shows the hydrogen flux through the Pd-membrane at $T = 528$ °C for a module with six fibres (membrane area 6.8 cm^2). The relation between the hydrogen flux and the difference of the hydrogen partial pressures can be described either with a linear or with a square root relation. This behaviour is due to the rather narrow range of the hydrogen partial pressure difference covered. The best fit can be achieved for a linear relation, which indicates mainly a rate limitation due to the surface reaction (eq. (8)), but it can also be due to membrane defects. The permeability coefficient of hydrogen $Q_{H_2,Henry}$ was found to be 9.5 $m^3/(m^2\,h\,bar)$. The separation factor $\alpha(H_2/N_2)$ is <18 corresponding to a permeability coefficient of nitrogen Q_{N_2} of 0.3 $m^3/(m^2\,h\,bar)$. A previously reported value for the permeability coefficient of hydrogen on this type of membrane at 400 °C was 8.8 $m^3/(m^2\,h\,bar)$ [16], Tong and Matsumura [14] found a permeability coefficient of 11.8 $m^3/(m^2\,h\,bar)$ and a separation factor of >1000 for individual Pd-coated fibres. From this comparison, it can be seen that the new multi-fibres modules developed in this study are less selective towards hydrogen than an individual fibre. Probably, the lower selectivity is due to the sealing of several fibres in the module. An additional possibility of the low separation factor compared with single fibres is the sealing of the module in the reactor.

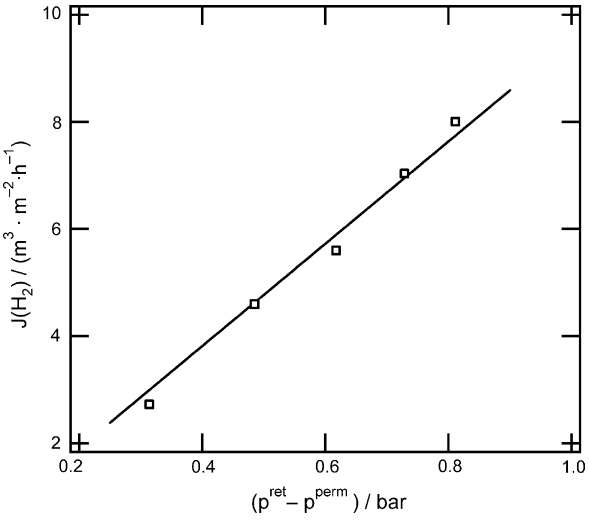

Fig. 3. Hydrogen flux vs. the difference of the partial pressure of hydrogen at $T = 528$ °C on the module with six fibres shown in Fig. 2.

Table 1
Comparison of calculated equilibrium data with experimental results (relative low value of GHSV: $3 \times 10^5\ h^{-1}$) at $T = 850$ °C for $H_2O/CH_4 = 3.3$

	Experiment	Calculation
Methane conversion (X_{CH}) (%)	96	100
Selectivity (S_{CO}) (%)	56	66
H_2/CO ratio	7	5

3.2. Kinetics

First, the equilibrium gas compositions leaving the reformer have been calculated using an established program (gaseq®). The equilibrium conversion and the selectivities were compared with the experimental results of the equilibrium measurements. As it can be seen from Table 1, the measured methane conversion (X_{CH}) and the carbon monoxide selectivity (S_{CO}) were slightly lower than the calculated equilibrium values.

The H_2O/CH_4 ratio influences the methane conversion because of a catalyst inhibition by steam [1]. Therefore, the H_2O content in the feed should be decreased (Table 2). On the other hand, a low H_2O/CH_4 ratio ($H_2O/CH_4 = 1.5$) favours the coke formation and leads to a fast deactivation of the catalyst [1]. In accordance with literature data [19], it was found that high steam content favours the production of carbon dioxide (Table 2).

The GHSV has been varied by changing the feed flow or the mass of the catalyst. As expected, the methane conversion decreases with increasing GHSV (Fig. 4). Unlike other reports [19], no linear relation between the methane conversion and the GHSV at low conversions could be found in this study. For higher temperatures at a given GHSV, the methane conversion is increased and the coke formation is reduced. The reduction of carbon formation with increasing temperature is contradictory to the literature [1,20]. In accordance with the literature [1], a higher H_2O/CH_4 ratio reduces the formation of coke. Both aspects follow from additional measurements at $T = 750$ °C which are not shown here. The coke formation is much faster at this low temperature of 750 °C compared to $T > 800$ °C and even with an H_2O/CH_4 ratio of 3.3 the catalyst deactivates after 5 h. Thus, at higher temperatures the SR-reaction can be

Table 2
Experimental conversion and selectivity at $T = 850$ °C and GHSV $3 \times 10^6\ h^{-1}$

H_2O/CH_4	Methane conversion (X_{CH}) (%)	Selectivity CO (S_{CO}) (%)	Selectivity CO_2 (S_{CO}) (%)
2.0	28.1	46.8	53.2
3.3	21.1	36.6	63.4
5.0	6.8	21.9	78.1

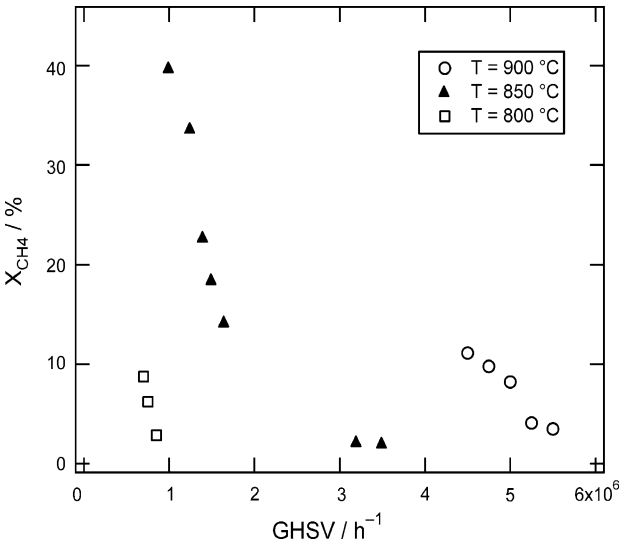

Fig. 4. Methane conversion vs. GHSV, H_2O/CH_4 ratio = 3.3.

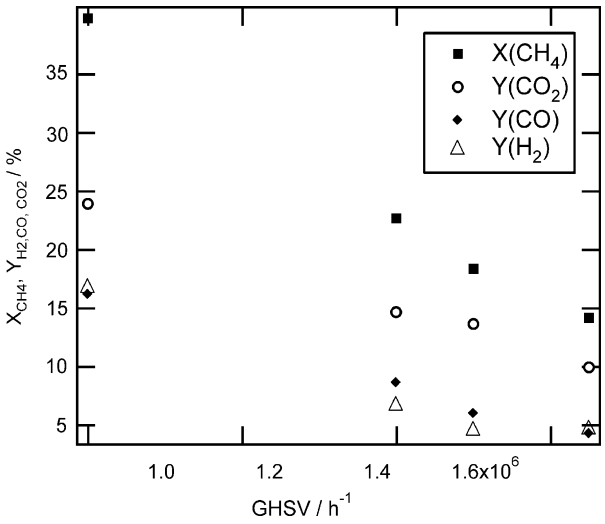

Fig. 6. Yield of hydrogen, carbon monoxide and carbon dioxide vs. GHSV; methane conversion vs. GHSV at $T = 850\ ^\circ C$ and $p = 1.7$ bar.

operated with a lower H_2O/CH_4 ratio, which leads to higher methane conversion with only marginal poisoning of the catalyst by coke.

The carbon monoxide selectivity increases with increasing methane conversion, which leads to the conclusion that carbon monoxide is not the primary product (Fig. 5). There seems to be no temperature dependency of the carbon monoxide selectivity.

In Fig. 6, the yield of hydrogen in the SR-process is shown as a function of the GHSV. As expected, the yield decreases with increasing GHSV. The low value of the yield (calculation analogous to eq. (11)) is due to the surplus of steam ($H_2O/CH_4 = 3.3$) in the reaction system.

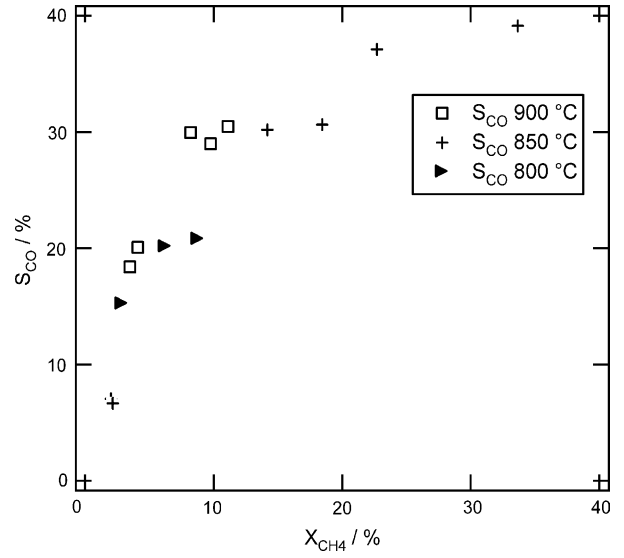

Fig. 5. Selectivity of carbon monoxide formation vs. methane conversion for H_2O/CH_4 ratio = 3.3.

3.3. Comparison of the simulated and experimental results

The kinetic mechanism of classical steam reforming was investigated very intensively in the last ten years [19,21]. For the simulation of the SR-process, a kinetic model developed for a Ni/α-Al_2O_3 catalyst (pore diameter of 0.15 mm and BET surfaces of 14.3 m^2/g) published in [18] was used. The corresponding rate expressions for the reaction eqs. (1)–(3) described by a Langmuir–Hinshelwood–Hougen–Watson approach are given by:

$$r_1 = \frac{k_1\left(p_{CH_4}\cdot\frac{p_{H_2O}^{0.5}}{p_{H_2}^{1.25}}\right)\cdot\left(1-\left(p_{CO}\cdot\frac{p_{H_2}^3}{K_1\cdot p_{CH_4}\cdot p_{H_2O}}\right)\right)}{\left(1+K_{CO}\cdot p_{CO}+K_H\cdot p_H^{0.5}+K_{H_2O}\cdot\frac{p_{H_2O}}{p_{H_2}}\right)^2}$$

$$r_2 = \frac{k_2\left(p_{CH_4}\cdot\frac{p_{H_2O}}{p_{H_2}^{1.75}}\right)\cdot\left(1-\left(p_{CO_2}\cdot\frac{p_{H_2}^4}{K_2\cdot p_{CH_4}\cdot p_{H_2O}^2}\right)\right)}{\left(1+K_{CO}\cdot p_{CO}+K_H\cdot p_H^{0.5}+K_{H_2O}\cdot\frac{p_{H_2O}}{p_{H_2}}\right)^2}$$

$$r3 = \frac{k_3\left(p_{CO}\cdot\frac{p_{H_2O}^{0.5}}{p_{H_2}^{0.5}}\right)\cdot\left(1-\left(p_{CO_2}\cdot\frac{p_{H_2}}{K_3\cdot p_{CO}\cdot p_{H_2O}}\right)\right)}{\left(1+K_{CO}\cdot p_{CO}+K_H\cdot p_H^{0.5}+K_{H_2O}\cdot\frac{p_{H_2O}}{p_{H_2}}\right)^2}$$

with r being the reaction rate of reactions (1)–(3), k the reaction rate constants, p_i the partial pressure of component i, K_1, K_2 and K_3 the reaction equilibrium constants of reactions (1)–(3) and K_i being the adsorption equilibrium constants of component i.

Due to the high steam/methane ratios the Boudouard reaction (eq. (4)) was not taken into account in the simulation. The dry-reforming (eq. (6)) is characterized by a secondary rule [19]. It further represents a linear combina-

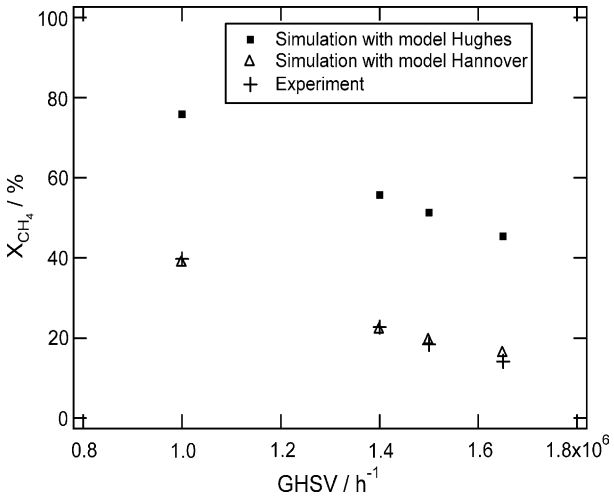

Fig. 7. Comparison of simulated CH_4 conversion and measured conversion for an H_2O/CH_4 ratio of 3.3.

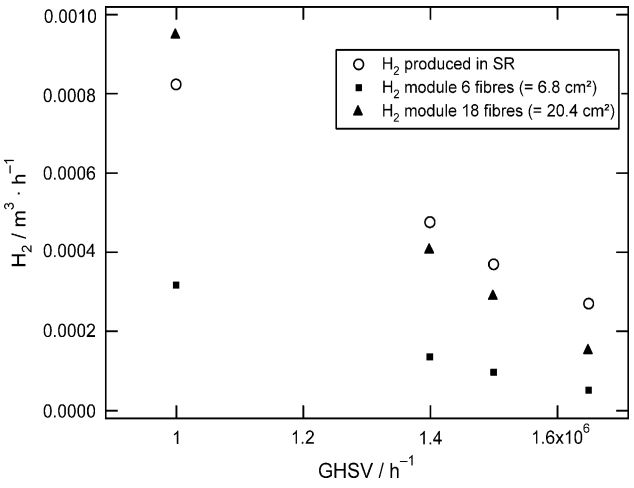

Fig. 8. Hydrogen produced in SR and possible hydrogen flux through the membrane for two different module geometries vs. GHSV. SR conditions: $T = 850\ ^\circ C$, $p = 1.7$ bar, $H_2O/CH_4 = 3.3$, $m_{catalyst} = 27.5$ mg; permeation conditions: at $T = 528\ ^\circ C$, $p_{ret} = 1$ bar, $p_{perm} = 0.002$ bar, $Q_{H_2} = 9.5\ m^3/(m^2\ h\ bar)$.

tion of reactions (eq. (1)) and (eq. (2)) [22]. An established one-dimensional, non-isothermal, non-isobaric (pressure drop expressed by the Ergun equation [23]), pseudo-homogeneous reactor model assuming steady-state conditions was used to describe the experimental data. The simulations were performed in MATLAB®. For the catalyst with higher BET surface area described by Hughes and co-worker [19], compared to the real BET surface of the experimentally investigated catalyst, the simulation gives a significantly higher conversion than the experimental data for the given GHSV. After modifying the Hughes model by the real BET surface of the catalyst used, the simulated and measured data fit quite well in the whole range of the considered space velocities (Fig. 7).

3.3.1. Compatibility study of membrane and catalyst

For the compatibility of the Pd-membrane and the SR-catalyst, the amount of hydrogen produced by SR was compared with the hydrogen flux through the membrane calculated from the experimentally determined permeability coefficient. This concept is similar to that of Dittmeyer et al. developed for the Pd-membrane supported dehydrogenation of hydrocarbons [9,24]. Fig. 8 shows the compatibility including the parameters of the catalytic SR-reactor. However, till now this model works only for a membrane reactor unit, which consists of the SR reactor and the separation unit behind the reactor. As discussed before, the hydrogen yield decreased with an increasing GHSV because of a decreasing methane conversion. This leads to a decreasing hydrogen partial pressure and thus to a lower driving force for the permeation and, consequently, to a lower hydrogen flux through the membrane. At a GHSV of $1.4 \times 10^6\ h^{-1}$ approximately 0.00048 m^3/h of hydrogen are produced. At the resulting hydrogen partial pressure a module with six fibres (6.8 cm^2) transports 0.00014 m^3/h hydrogen. In contrast, a module with 18 fibres (20.4 cm^2) could transport 0.00041 m^3/h. For the extraction of the total hydrogen produced, a module with a membrane surface area >20 cm^2 is needed. However, at a GHSV of $1.0 \times 10^6\ h^{-1}$ the hydrogen amount is 0.00082 m^3/h. Under these conditions a module with six fibres will transport 0.00032 m^3/h and a module with 18 fibres will transport 0.00095 m^3/h and, therefore, is able to extract the total amount of hydrogen produced from the reaction zone. As shown in [25], from Fig. 8 the necessary membrane area and/or the number of hollow fibres in the membrane module for a desired GHSV can be estimated.

Desirable is a membrane reactor with a combined reaction and separation zone. In this reactor, the catalyst will be placed around the hollow fibres so that the fibres can extract the hydrogen produced through the SR. For this reactor, it is necessary to adhere the extraction of hydrogen from the reaction zone. This will lead to an increase of the conversion and an increase of yield of hydrogen. Furthermore, the inhibiting or poisoning effect of products like carbon monoxide or carbon dioxide has to be investigated. A possible inhibiting effect of carbon monoxide could be compensated by enlarging the membrane area.

4. Conclusions

With the study of the steam reforming process and the hydrogen permeation through a Pd-membrane the compatibility of hydrogen transfer and kinetics of steam reforming process of a given state of the art catalyst has been examined. For a certain GHSV, the membrane area needed can be estimated using the permeability coefficient and the produced hydrogen. From the kinetic studies, the optimum reaction parameters for the two-coupled processes of catalytic reaction and permeation in the membrane reactor can be determined. Furthermore, this simulation provides the basis for a more detailed design of the membrane reactor.

Acknowledgement

The authors thank the German Catalysis Research Network CONNECAT for financial support.

References

[1] K. Kochloefl, Steam reforming, in: G. Ertl, H. Knözinger, J. Weitkamp (Eds.), Handbook of Heterogenous Catalysis, vol. 1, VCH, Weinheim, 1997, p. 1819.
[2] M. Oertel, J. Schmitz, W. Weirich, D. Jendryssek-Neumann, R. Schulten, Chem. Eng. Technol. 10 (1987) 248.
[3] E. Kikuchi, Cattech 1 (1997) 67.
[4] S. Uemiya, N. Sato, H. Ando, T. Matsuda, E. Kikuchi, Appl. Catal. A 67 (1991) 223.
[5] B.A. Raich, H.C. Foley, Appl. Catal. A 129 (1995) 167.
[6] N. Itoh, Catal. Today 25 (1995) 351.
[7] S.L. Jørgensen, P.E.H. Nielsen, P. Lehrmann, Catal. Today 25 (1995) 303.
[8] H. Amandusson, L.G. Ekedahl, H. Dannetun, Appl. Surf. Sci. 153 (2000) 259.
[9] R. Dittmeyer, V. Höllein, K. Daub, J. Mol. Catal. A Chem. 173 (2001) 135.
[10] J. Shu, B.P.A. Grandjean, A. van Neste, S. Kaliaguine, Can. J. Chem. Eng 69 (1991) 1036.
[11] R.C. Hurlbert, J.O. Konecny, J. Chem. Phys. 34 (1961) 655.
[12] G.D. Berkheimer, R.E. Buxbaum, J. Vac. Sci. Technol. 3 (1985) 412.
[13] W.J. Koros, Y.H. Ma, T. Shimidzu, J. Membr. Sci. 120 (1996) 149.
[14] J. Tong, Y. Matsumura, Chem. Commun. 21 (2004) 2460.
[15] J.E. Dobo, T.E. Graham, U.S. Patent 4175153, 1979.
[16] X.L. Pan, N. Stroh, H. Brunner, G.X. Xiong, S.S. Sheng, J. Membr. Sci. 226 (2003) 111.
[17] X.L. Pan, G.X. Xiong, S.S. Sheng, N. Stroh, H. Brunner, Chem. Commun. (2001) 2536.
[18] X.L. Pan, N. Stroh, H. Brunner, G.X. Xiong, S.S. Sheng, Sep. Purif. Technol. 32 (2003) 265.
[19] K. Hou, R. Hughes, Chem. Eng. J. 82 (2001) 311.
[20] Z. Chen, Y. Yan, S.S.E.H. Elnashaie, Chem. Eng. Sci. 59 (2004) 1965.
[21] J. Xu, G.F. Froment, AIChE J. 35 (1989).
[22] A.M. De Groote, G.F. Froment, Appl. Catal. A 138 (1996) 245.
[23] S.S.E.H. Elnashaie, S.S. Elshishini, Modelling, simulation and optimization of industrial fixed bed catalytic reactors, in: R. Hughes (Ed.), Topics in Chemical Engineering, vol. 7, Gordon and Breach Science Publishers, 1993.
[24] P. Quicker, V. Höllein, R. Dittmeyer, Catal. Today 56 (2000) 21.
[25] J.M. van de Graaf, M. Zwiep, F. Kapteijn, J.A. Moulijn, Appl. Catal. A 178 (1999) 225.